CHEMICAL ENGINEERING TRANSACTIONS
VOL. 57, 2017
A publication of AIDIC
The Italian Association of Chemical Engineering
Online at www.aidic.it/cet
Guest Editors: Sauro Pierucci, Jiří Jaromír Klemeš, Laura Piazza, Serafim Bakalis

ISBN 978-88-95608- 48-8; **ISSN** 2283-9216

Oxidative Degradation of Organic Pollutants by a New Hybrid Titania Based Gel-Derived Material with Stable Radical Species

Domenico Pirozzi*[a], Filomena Sannino[b], Biancamaria Pietrangeli[c], Maria Abagnale[a], Claudio Imparato[a], Gaetano Zuccaro[a], Luciana Minieri[a], Antonio Aronne[a]

[a]Dipartimento di Ingegneria Chimica, dei Materiali e della Produzione Industriale (DICMAPI) - Università Federico II di Napoli, P.le Tecchio, 80, 80125 Napoli, Italia
[b]Dipartimento di Agraria - Università Federico II di Napoli, via Università, 100 – 80055 Portici (NA)
[c] Dipartimento Innovazioni Tecnologiche e Sicurezza degli Impianti, Prodotti ed Insediamenti Antropici. INAIL Ricerca, Via Alessandria, 220/E, 00198 Roma
dpirozzi@unina.it

A TiO_2–based hybrid material (HSGT), obtained by a sol–gel route wholly performed in air at room temperature, was used as catalyst for the oxidative degradation of 2,4-dichlorophenol (2,4-DCP), 4-chlorophenoxyacetic acid (4-CPA) and phenanthrene (PHE). Acetylacetonate ligands, used as complexing/sensitizing molecules, was added directly to the solution containing the precursors of titanium. In the presence of air, the acetylacetonate ligands on the HSGT surface were able to generate stable superoxide radicals, as demonstrated by EPR measurements. The presence of superoxide radicals correlated to the catalytic activity of HSGT. ThDue to the stability of the free radicals, HSGT can be considered a promising catalyst for the degradation of organic pollutants.

1. Introduction

Many research efforts are being devoted to develop efficient methods for the elimination of recalcitrant pollutants from soils and waters. Among the technologies that involve the use of inorganic catalysts, advanced oxidation processes (AOPs) have been widely used for the wastewaters treatment over the last few decades (Sievers, 2011; Rosa et al., 2012; Capocelli et al., 2013). In particular, the photocatalytic exploitation of TiO_2-based materials offers different environmental applications, such as the oxidative degradation of organic pollutants, the solar energy conversion in processes as water spitting, the CO_2 reduction and the dye sensitized solar cell production (Kumar and Devi, 2011; Sima and Hasal, 2013; Zhang et al., 2014). Yet, the wide band-gap of TiO_2 (~3.2 eV for anatase and ~3.0 eV for rutile) leads to a reduced absorption of solar light radiation (less than 5%) in the semiconductor-assisted photocatalysis. Consequently, a growing interest is devoted to extending the optical response of titanium oxide in the visible region.
Doping with metallic or non-metallic elements is a common way to modify large band-gap semiconductors, as it generates intermediate energy states in the lattice (Kumar and Devi, 2011; Zhang et al., 2014). The electronic transitions between the semiconductor bands and dopant levels occur by absorbing visible light. So far, TiO_2 has been activated in the visible by coupling with others semiconductors having lower band-gap (Tada et al., 2014; Pelaez et al., 2012). In addition, Co_2O_3–TiO_2 active in the degradation of pollutants both in the dark and under visible light irradiation has showed significant thermocatalytic activity (Jin et al., 2013). The synthesis of TiO_2-based hybrid heterostructure nanocomposites has recently allowed a more efficient utilization of the solar spectrum (Bai et al., 2015).
The surface absorption of organic molecules offers a way to enable visible light activation of TiO_2 crystalline nanoparticles as well as of other wide band-gap semiconductors. The activation can occur in two different mechanisms. In the first one, relatively large dye molecules are adsorbed onto an oxide surface. In this case

the electronic transition between HOMO and LUMO of dye molecules occurs by absorbing a visible light photon. Electrons are then injected from the excited dye molecule into the conduction band of the semiconductor. This mechanism has been extensively studied in common dyesensitized solar cells (Vinodgopal et al., 1996). In the second mechanism, relatively small organic molecules adsorbed on the oxide surface form a charge transfer complex that absorbs in the visible region at energy lower than either the chelating molecules or the oxide particles. In this case, direct injection of an electron from the ground state of the molecule into the conduction band of the oxide occurs without involvement of any excited molecular state. This direct charge transfer from the HOMO of the adsorbed molecule to the conduction band (CB) of the oxide, has to be seen as ligand-to-metal charge transfer (LMCT) process (Kumar and Devi, 2011; Zhang et al., 2014). Among electron rich ligands are the oxygen-based bidentate ligands such as salicylic acid, dopamine, catechol and acetylacetone, these molecules that form a CT state with semiconductors also show surface enhanced Raman scattering (SERS) through the chemical effect (Finkelstein-Shapiro et al., 2013). To achieve visible light sensitization, usually dye or small sensitizing molecules are adsorbed on previously prepared TiO_2 crystalline nanoparticles.

In this paper a hybrid TiO_2–acetylacetonate material (HSGT) was synthesized by a sol–gel route. Contrary to the usual practice, the complexing/sensitizing molecules were added directly into the solution containing the precursor of titanium. A porous gel-derived material was obtained, with acetylacetonate molecules strongly linked on its surface, and a significantly lower band-gap (2.5 eV). The presence on its surface of stable free radicals made this material an active catalyst in organic pollutants degradation.

In order to demonstrate the catalytic efficiency of HSGT in environmental remediation processes, three common pollutants were adopted as model compounds, namely: 2,4-dichlorophenol (2,4-DCP), a by-product from herbicide utilization, 4-chlorophenoxyacetic acid (4-CPA), an herbicide classified as potential groundwater contaminants by U.S. EPA, and phenanthrene (PHE), a typical three-ring polycyclic aromatic hydrocarbon.

2. Materials and Methods

2.1 Materials

Titanium(IV) propoxide (70 wt.% in 1-propanol), acetylaceton (>99%), and 1-propanol (>99.80%) were provided by Sigma-Aldrich. 2,4-dichlorophenol (2,4-DCP) 4-chlorophenoxyacetic acid (4-CPA) and phenanthrene (PHE) were purchased from Sigma-Aldrich Chemical Co. (Poole, Dorset, UK; 99.0% purity). All solvents were of HPLC grade (Carlo Erba, Milan, Italy) and were used without further purification.

2.2 Sol-gel synthesis

The hybrid sol–gel TiO_2 (HSGT) was prepared by a sol–gel route using titanium(IV) n-butoxide (97+%), acetylacetone (Hacac) (99+%), 1-propanol (99.80+%) and hydrochloric acid (37 wt%) provided by Sigma-Aldrich. All the reagents were used without further purication. A solution containing 10 mL of titanium(IV) n-butoxide (29.1 mmol), 1.20 mL of acetylacetone (11.6 mmol) and 3.87 mL of 1-propanol (51.8 mmol) was prepared and stirred for a few minutes at 50 °C. A second solution containing 5.27 mL of distilled water (291 mmol), 7.0 mL of 1-propanol (93.6 mmol) and one drop of HCl (37 wt%) was then prepared and mixed with the first one. The resulting molar ratioTi : Hacac : propanol : water was 1 : 0.4 : 5 : 10. The solution obtained was vigorously stirred at 50 °C for about 5 min, until the gelation occurred. A homogeneous yellow colored gel was obtained. The gel was left at room temperature for 24 h and then dried under air flow at 30 °C until constant weight, obtaining a porous amorphous material. A reference TiO_2 matrix (SGT) was also prepared in similar conditions except for the lack of acetylacetone in the solution of the Ti precursor. Consequently, when the hydro-alcoholic solution was added to the precursor solution, the instantaneous formation of a particulate gel took place.

2.3 Structural characterization of the sol-gel matrix

Gel-derived TiO_2 material, HSGT, was characterized by Electron Paramagnetic Resonance (EPR). The powder samples were analyzed using an X-band (9 GHz) Bruker Elexys E-500 spectrometer (Bruker, Rheinstetten, Germany). The capillary containing the sample was placed in a standard 4 mm quartz sample tube. The temperature of the sample was regulated at 25 °C and maintained constant during the measurement by blowing thermostated nitrogen gas through a quartz Dewar. The instrumental settings were as follows: sweep width, 140 G; resolution, 1024 points; modulation frequency, 100 kHz; modulation amplitude, 1.0 G; time constant, 20.5 ms. EPR spectra were measured with attenuation of 10 dB to avoid microwave saturation of resonance absorption curve. Several scans, typically 32, were accumulated to improve the signal-tonoise ratio. The g values and the spin density of the samples were evaluated by means

of an internal standard, Mn^{2+}-doped MgO, prepared by modifying a synthesis protocol reported in the Literature (Yordanova et al., 1999) The reactants were purchased from Sigma-Aldrich. MgO and $MnSO_4$ of high purity (99.99%) were used in order
to prepare two aqueous solutions of $Mg(NO_3)_2$ and $Mn(NO_3)_2$, by adding nitric acid with a molar excess of 20% in respect to the metal. Proper aliquots of these solutions were mixed and a third aqueous solution of $(NH_4)_2CO_3$ was added slowly. In order to assure a complete conversion of the nitrates into the carbonates, a large excess of $(NH_4)_2CO_3$ was employed, due to the acidic environment. The neutralization of the acidic solution was followed by the precipitation of the mixed carbonate. The precipitate was filtered and resuspended in 100 mL of distilled water in order to remove the ammonium cations, whose presence could interfere with EPR measurements. After 15 minutes, the mixed carbonate was filtered, washed twice with distilled water and dried in oven at 50 °C for 24 hours. The solid was calcined at 900 °C for 4 hours in a slightly reducing atmosphere (97% N_2 and 3% H_2 vol). The Mn/Mg molar ratio in the final product was assessed to be 0.05% by ICP-MS analysis.

2.4 Removal kinetics

All the kinetic experiments were carried out in batch conditions in the dark, in a rotary shaker at room temperature. Blanks of herbicides were analyzed in order to check the possible sorption to vials. Due to the different solubility of the contaminants, the tests were performed adopting different initial concentrations of 2,4-DCP (0,3 mM), 4-CPA (0,2 mM), and PHE (5.6 10^{-3} mM). Kinetic experiments were performed incubating suitable amounts of HSGT matrix with 2 cm^3 of contaminant solution for different incubation times. All the experiments were carried out in a 20 mL capped glass test tube. The inside air volume assured an oxygen reservoir, largely exceeding the stoichiometric amount required for the full oxidation of contaminants. Therefore, the tests can be considered as made at constant O_2 concentration. After incubation, the samples were centrifuged at 7000 rpm for 20 minutes and the supernatants were analyzed.
The analysis of PHE, 2,4-DCP and 4-CPA was carried out by an Agilent 1200 Series HPLC apparatus (Wilmington U.S.), equipped with a DAD and a ChemStation Agilent Software. A Macherey-Nagel Nucleosil 100-5 C18 column (stainless steel 250 x 4 mm) was utilized.
When analysing 2,4-DCP, the mobile phase, a binary system of 65 : 35 acetonitrile : water (1% acetic acid), was pumped at 1 cm^3 min^{-1} flow in isocratic mode. The detector was set at 280 nm. When analysing 4-CPA, the mobile phase, a binary system of 40 : 60 acetonitrile : phosphate buffer (0.1%. pH 2.5), was pumped at 1 cm^3 min^{-1} flow in isocratic mode. The detector was set at 283 nm. In all cases the injection volume was 20 μL.
The conditions adopted for PHE analysis are described in detail elsewhere (Sannino et al, 2014).
The percent removal (η) of all contaminants was calculated by the following balance equation:

$$\eta = \frac{C_0 - C}{C_0} * 100 \qquad (1)$$

where C_0 and C are the concentration of PHE (mg L^{-1}) at the start and at the end of the incubation, respectively.

3. Results and Discussion

3.1 Removal kinetics of pollutants

The removal kinetics of 2,4-dichlorophenol (2,4-DCP) and 4-chlorophenoxyacetic acid (4-CPA) in the presence of HSGZ is described in Figure 1. In both cases the concentration-time profiles obtained tend asymptotically to zero, demonstrating that the overall catalytic process irreversibly tends towards a complete removal of the contaminants.
Further experimental tests, made adopting HSGZ as catalyst and PHE as model compound, showed the complete removal of the contaminant in about 60 min (data not shown).
A physico-chemical model was developed to clarify the mechanism of HSGZ-catalyzed removal of contaminants. Adopting a pseudo-first-order kinetic model and a pseudosecond-order kinetic model (Ozacar and Sengil, 2006) to describe the experimental data in Figure 1, low correlation coefficients r^2 were obtained. Consequently, an alternative physico-mathematical model, previously developed by our group (Aronne et al., 2012) was used to elaborate the data, describing the removal of contaminants as a two-stage process:

- a reversible, first-order adsorption of contaminants on the HSGZ;
- a subsequent conversion of contaminants, catalytically driven by HSGZ surface groups, to degradation products;

The model is synthetically described by the scheme:

$$C_{sol} \underset{k_{-1}}{\overset{k_1}{\rightleftharpoons}} C_{ads} \xrightarrow{k_2} P \qquad (2)$$

where C_{ads} is the concentration of adsorbed herbicide, P indicates the degradation products, k_1 and k_{-1} are the direct and inverse first-order kinetic constants of the herbicide sorption, and k_2 is the first-order kinetic constants of the herbicide degradation.
The mass balances applied to the chemical species involved in model (2) yield concentration−time profiles describing the herbicide removal by double-exponential curves:

$$C_{sol}(t) = A \cdot e^{-\lambda_1 t} + B \cdot e^{-\lambda_2 t} \qquad (3)$$

where C_{sol} is the herbicide concentration in the liquid phase (mmol L^{-1}), and t the time (h).
The Mathematical model (3) could satisfactorily be used to interpolate the experimental data. The interpolating curves are dashed in Figure 1.

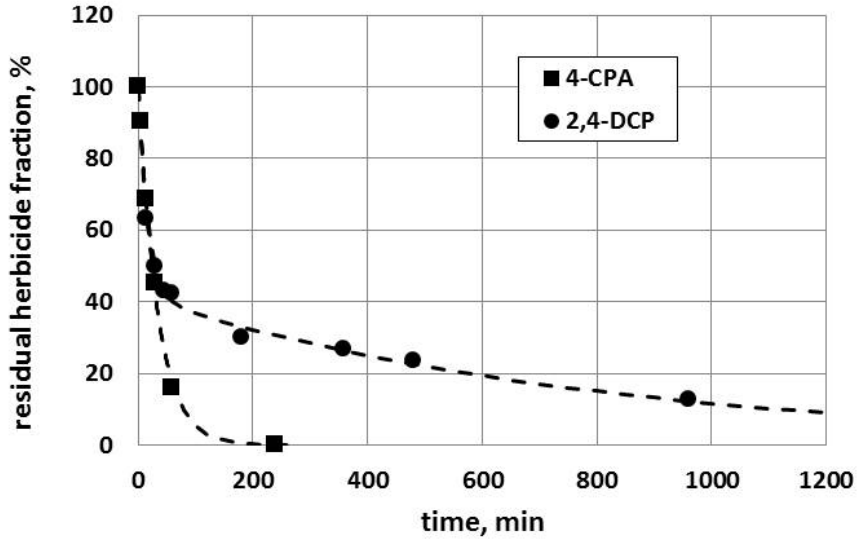

Figure 1: Kinetics of 2,4-DCP (●) and 4-CPA (■) removal in the presence of HSGT matrix. The experimental procedure is described in the Materials and Methods paragraph. The interpolation curves have been obtained using the mathematical model (3). The estimated parameters are reported in Table 1.

The estimated values of the model parameters, reported in the Table 1 together with the correlation coefficients, demonstrate that the curve pertaining to 4-CPA removal could be modeled as a simple exponential function. For this reason, the corresponding estimates of the parameters A and λ_1 are not reported.

Table 1: estimates of parameters and of the correlation coefficient (R^2) obtained from the mathematic model (3)

contaminant	A (mmol/L)	B (mmol/L)	λ_1 (1/min)	λ_2 (1/min)	R^2
2,4-DCP	0,17	0,13	$6{,}07 \cdot 10^{-2}$	$1{,}28 \cdot 10^{-3}$	0,92
4-CPA	na	1	na	$2{,}90 \cdot 10^{-2}$	0.89

3.2 Characterization by EPR spectroscopy

In order to reveal the presence of paramagnetic species, the hybrid gel-derived TiO_2 material (HSGT) as well as the reference titania gel without acetylacetone (SGT) were characterized by EPR spectroscopy. Each

measurement was repeated after 12 h leaving the sample in the sample-holder of the spectrometer to avoid any light exposure.
The EPR spectrum of the HSGT powder at room temperature, reported in Figure 2 (curve a), presents a complex anisotropic lineshape, that is correlated to the presence of stable radicals adsorbed on the HSGT surface. The spectrum does not show any signal ascribable to Ti^{3+} ions (Chiesa et al., 2013), thus excluding the presence of a significant amount of this species in the sample. Consequently, it can be inferred that also in the case of HSGT the spectrum is due to stably adsorbed $\bullet O_2^-$ species.
On the contrary, the EPR spectrum pertaining to the SGT presents a virtually isotrophic lineshape (not shown). This result demonstrates that acetylacetone ligands play a key role in generating and stabilizing the superoxide radical anions.

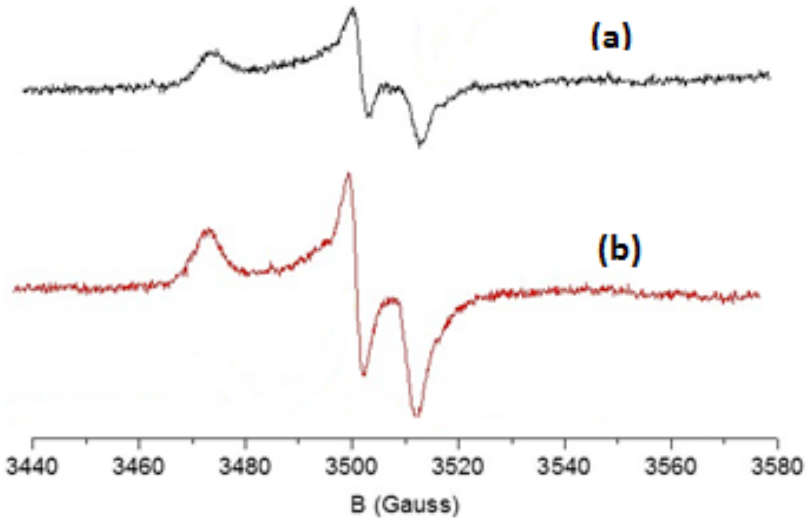

Figure 2: EPR spectra of HSGT: as-dried (a), and regenerated after 12 months (b). Spectra recorded at room temperature.

3.3 Storage inactivation and regeneration of the catalyst

After a 12 months storage in the absence of light, the HSGT lost almost completely its catalytic activity towards 2,4-DCP, 4-CPA and PHE. The EPR spectrum of HSGT after storage presents an isotrophic lineshape (not shown), demonstrating the absence of paramagnetic species.
However, upon a 24-h incubation in distilled water, the catalytic activity of HSGT was almost completely recovered. In all the experimental tests, the regenerated catalyst showed more than 90% of its initial catalytic activity (data not shown). Correspondingly, the EPR spectrum of the regenerated HSGT (Figure 2, curve b) showed an anisotropic lineshape, that can be correlated to the presence of stable superoxide radical anions.

4. Conclusions

A TiO_2–acetylacetonate hybrid material (HSGT) was synthesized by a sol–gel route, using acetylacetonate molecules as complexing/sensitizing molecules. Contrary to the usual practice, the complexing compound was added directly to the solution containing the precursors of titanium. The porous-gel derived material obtained was amorphous, with acetylacetonate molecules strongly linked on its surface. In the presence of air, the acetylacetonate ligands on the HSGT surface generated and stabilized superoxide radicals. The presence of stable free radicals was ascertained by EPR. The degradation of different organic pollutants, namely 2,4-dichlorophenol, 4-chlorophenoxyacetic acid and phenanthrene, was carried out using HSGT as catalyst.
The experimental results, obtained on the fresh material, after a 12-month storage, and after the subsequent regeneration, demonstrate that there is a clear correspondance between the formation of stable superoxide radical anions and the catalytic activity of the HSGT.

References

Aronne A., Sannino F., Bonavolontà S.R., Fanelli E., Mingione A., Pernice P., Spaccini R., Pirozzi, D., 2012, Use of a New Hybrid Sol−Gel Zirconia Matrix in the Removal of the Herbicide MCPA: a Sorption/Degradation Process, Environ. Sci. Technol., 46, 1755−1763.

Bai S., Wang L., Chen X., Du J., Xiong Y., 2015, Chemically exfoliated metallic MoS_2 nanosheets: A promising supporting co-catalyst for enhancing the photocatalytic performance of TiO_2 nanocrystals, Nano Res., 8, 175–183.

Capocelli M., Prisciandaro M., Musmarra D., Lancia A., 2013, Understanding the Physics of Advanced Oxidation in a Venturi Reactor, Chemical Engineering Transactions, 32, 691-696.

Chiesa M., Paganini M. C., Livraghi S., Giamello E., 2013, Charge trapping in TiO_2 polymorphs as seen by Electron Paramagnetic Resonance spectroscopy, Phys. Chem. Chem. Phys., 15, 9435–9477.

Finkelstein-Shapiro D., Hurst Petrosko S., Dimitrijevic N.M., Gosztola D., Gray K.A., Rajh T., Tarakeshwar P., Mujica V., 2013, CO2 preactivation in photoinduced reduction via surface functionalization of TiO2 nanoparticles, The journal of physical chemistry letters, 4, 475–479.

Jin Q., Yamamoto H., Yamamoto K., Fujishima M., Tada H., 2013, Simultaneous induction of high level thermal and visible-light catalytic activities to titanium(IV) oxide by surface modification with cobalt(III) oxide clusters, Phys. Chem. Chem. Phys., 15, 20313–20319.

Kumar S. G., Devi L. G., 2011, Review on modified TiO2 photocatalysis under UV/visible light: selected results and related mechanisms on interfacial charge carrier transfer dynamics, J. Phys. Chem. A, 115, 13211–13241.

Ozacar M., Sengil I.A., 2006, A Two Stage Batch Adsorber Design for Methylene Blue Removal to Minimize Contact Time, J. Environ. Manag., 80, 372−379.

Pelaez M., Nolan N.T., Pillai S.C., Seery M.K., Falaras P., Kontos A.G., Dunlop P.S.M., Hamilton J.W.J., Byrne J.A., O'Shea K., Entezari M.H., Dionysiou D.D., 2012, A Review on the Visible Light Active Titanium Dioxide Photocatalysts for Environmental Applications, Appl. Catal., B, 125, 331–349.

Rosa J.M., Tambourgi E.P., Curvelo Santana J.C., 2012, Reuse of Textile Effluent Treated with Advanced Oxidation Process by UV/H2O2, Chemical Engineering Transactions, 26, 207-212.

Sacco O., Vaiano V., Changseok H., Sannino D., Dionysiou D.D., Ciambelli P., 2015, Long Afterglow Green Phosphors Functionalized with Fe-N Doped TiO2 for the Photocatalytic Removal of Emerging Contaminants, Chemical Engineering Transactions, 43, 2107-2112.

Sannino F., Pirozzi D., Vitiello G., D'Errico G., Aronne A. Fanelli E., Pernice P., 2014, Oxidative degradation of phenanthrene in the absence of light irradiatiion by hybrid ZrO2-acetylacetonate gel-derived catalyst, Applied Catalysis B Environmental, 156–157, 101–107.

Sievers M., 2011, Advances Oxidation Processes. In: Treatise on Water Science; Elsevier: Amsterdam, the Nederlands, 4, 377−408.

Sima J., Hasal P., 2013, Photocatalytic Degradation of Textile Dyes in a TiO_2/UV System, Chemical Engineering Transactions, 32, 79-84.

Tada H., Jin Q., Iwaszuk A., Nolan M., 2014, Molecular-Scale Transition Metal Oxide Nanocluster SurfaceModified Titanium Dioxide as Solar-Activated Environmental Catalysts, J. Phys. Chem. C,118, 12077–12086.

Vinodgopal K., Wynkoop D., Kamat P.V., 1996, Environmental Photochemistry on semiconductor surfaces: A photosensitization approach for the degradation of a textile azo dye, Acid Orange 7. Environ. Sci. Technol., 30, 1660-1666.

Yordanova V. N., Gancheva V., Pelova V. A., 1999, Studies on some materials suitable for use as internal standards in high energy EPR dosimetry, J. Radioanal. Nucl. Chem., 240, 619–622.

Zhang G., Kim G., Choi W., 2014, Visible light driven photocatalysis mediated via ligand-to-metal charge transfer (LMCT): an alternative approach to solar activation of titania, Energy Environ. Sci., 7, 954–966.